Shape coexistence close to $N=50$ in the neutron-rich isotope ^{80}Ge investigated by IBM-2*

Da-Li Zhang(张大立)[1] Cheng-Fu Mu(穆成富)[2]
Department of Physics, Huzhou University, Huzhou 313000, China

Abstract: The properties of the low-lying states, especially the relevant shape coexistence in ^{80}Ge, close to one of most neutron-rich doubly magic nuclei at $N=50$ and $Z=28$, have been investigated within the framework of the proton-neutron interacting model (IBM-2). Based on the fact that the relative energy of the d neutron boson is different from that of the proton boson, the calculated energy levels of low-lying states and $E2$ transition strengths can reproduce the experimental data very well. Particularly, the first excited state 0_2^+, which is intimately related to the shape coexistence phenomenon, is reproduced quite nicely. The $\rho^2(E0,0_2^+\to 0_1^+)$ transition strength is also predicted. The experimental data and theoretical results indicate that both collective spherical and γ-soft vibration structures coexist in ^{80}Ge.

Keywords: ^{80}Ge, low-lying states, $E0$ transition strengths, shape coexistence, IBM-2

PACS: 21.10.Re, 21.60.Fw, 27.50.+e **DOI:** 10.1088/1674-1137/42/3/034101

1 Introduction

Shape coexistence is a peculiar nuclear phenomenon where two or more states occur in the same nucleus within a very narrow energy range at low excitation energy [1]. The shape coexistence phenomenon is often found close to or at the shell closures, where deformed intruder configurations coexist with spherical shapes based on multiparticle-hole excitations across the closed shell in the nuclear chart, from light nuclei to heavy nuclei [2–4]. The presence of low-lying 0^+ states as the first excited state in even-even nuclei is one of the signatures of shape coexistence [2, 5], which plays an important role in our understanding of the shape changes of nuclear structure in exotic nuclei.

In recent years, radioactive isotope beams have been developed, giving access to exotic nuclei far from stability in both the neutron-deficient and neutron-rich regimes [1, 6–10]. In neutron-rich nuclei, empirical evidence of shape coexistence has been observed along $N=20$, $N=28$ and the subshell gap $N=40$, see Refs. [2,3] for reviews. A lot of theoretical work has been developed to investigate shape coexistence and shape phase transitions, such as the interacting-boson model [11, 12], the shell model [13] and projected shell model [14, 15], and the self-consistent relativistic mean-field theory [16]. Shape coexistence in nuclei close to the supposedly doubly magic nucleus $^{78}_{28}$Ni$_{50}$ is the focus of intense experimental and theoretical research (cf., for example Refs. [4, 17, 18] and references therein), because the study of shape coexistence in this region will help us to differentiate the single-particle effect from quadrupole collective motion across $N=50$. More recently, the technique of β-delayed electron-conversion spectroscopy has been applied to study the ^{80}Ge nucleus. In Ref. [18], an electric monopole $E0$ transition was observed for the first time, which points to an intruder 0_2^+ state at 639(1) keV. The new state 0_2^+ is much lower than the 2_1^+ level in ^{80}Ge. This implies that shape coexistence might exist near the most neutron-rich doubly magic nucleus at $N=50$ and $Z=28$, giving an insight into the mechanism of shape coexistence close to the major neutron shell closure at $N=50$.

It is well known that the low-lying structure of Ge isotopes shows the coexistence of different shapes along the long isotopic chain, characterized by prolate-oblate and spherical-deformed competition. Close to the β-stability line, the shape transition of Ge isotopes is a drastic evolution from nearly spherical in ^{72}Ge to slight prolate in ^{74}Ge or even triaxiality in ^{76,78}Ge [19–22] and ^{84,86,88}Ge [23]. In the neutron-rich region, the $B(E2)$ behavior has a smooth decrease toward $N=50$ [24]. Both the shape transition from spherical to weakly deformed and the coexistence of different types of deformation might occur

Received 23 October 2017, Published online 29 January 2018
∗ Supported by National Natural Science Foundation of China (11475062, 11647306, 11147148)
1) E-mail: zdl@zjhu.edu.cn
2) E-mail: muchengfu@zjhu.edu.cn

in these isotopes [25]. A rich variety of shapes and shape coexistence in Ge isotopes provides a challenging testing ground for theoretical models. The Skyrme-Hartree-Fock (SHF) and Gogny Hartree-Fock-Bogoliubov (HFB) models imply that most Ge isotopes show the features of soft triaxial deformation [26]. The self-consistent total-Routhian-surface calculations show there are shape phase transitions from oblate deformation, through triaxial deformation, to prolate deformation in even-mass $^{64-80}$Ge isotopes [20, 27]. Nuclear density functional theory has been used to investigate the structural evolution from weakly triaxial deformation in ^{74}Ge to γ soft deformation in ^{78,80}Ge, and finally to a spherical shape in ^{82}Ge [28]. The multi-quasiparticle triaxial projected shell model demonstrates that ^{76}Ge exhibits a rigid γ deformation in its low-lying states. It is rare for a nucleus to have this kind of nuclear structure. However, its neighboring nuclei, such as the ^{70,72,74,78,80}Ge isotopes, show different γ-soft features [29]. Moreover, for ^{80}Ge, because of a subtle balance between quadrupole terms and the pairing term in the interaction, each term of the interaction governs two coexisting systems respectively: one for the quasiparticle type and the other for the collective triaxial type [30]. These interactions determine the features of ^{80}Ge.

In Ref. [31], the authors discussed the general properties of low-lying states of the even-even Ge isotopes through the interacting boson model (IBM-1). IBM-1 does not distinguish neutron pairs and proton pairs [32]. The calculation results reproduced the available experimental data, and suggested that there exist shape transitions from the mixture of $U(5)$, $SU(3)$ and $O(6)$ symmetry to the mixture of $U(5)$ and $O(6)$ and finally to $U(5)$ symmetry along the even-even isotopes of $^{64-78}$Ge [31]. Meanwhile, the authors of Ref. [33] satisfactorily reproduced the available experimental information on the energy spectum, $E2$ transition and quadrupole moments for the even-mass $^{68-76}$Ge through the proton-neutron interacting boson model (IBM-2). In IBM-2, proton bosons and neutron bosons are treated independently as different degree of freedom, and mixing of their configurations is introduced [32]. Furthermore, the energy levels, $E2$ and $M1$ transition properties of even-even isotopes $^{64-68}$Ge were analyzed through the IBM model with isospin (IBM-3) in Ref. [34].

Very recently, shape coexistence and shape transitions in the even-even nuclei $^{66-94}$Ge were calculated by using the IBM-1 [35], where the authors applied a self-consistent mean-field method on the basis of the Gogny-D1M energy density functional theory. This calculation agreed with the known experimental data of these nuclei. However, their calculated energy levels for the states $E(0_2^+)$ and $E(2_2^+)$ are a little higher than the experimental data, especially for ^{80}Ge. The reason is that the proton-neutron pairing effects cannot be neglected in this case. The IBM-2 without introducing configuration mixing has been used to investigate shape coexistence in some nuclei in the $A\sim100$ mass region [36, 37], and in the neutron-deficient isotopes ^{74,76}Kr [38]. The numerical calculations are in good agreement with the recent experimental values for the low-lying energy spectrum, and the key sensitive quantities such as the quadrupole shape invariants and the $B(E2)$ transition strength branch ratios. In particular, the calculation reproduces the low-lying 0_2^+ state, which is intimately related to the shape-coexistence phenomenon, quite well. However, there is no detailed investigation on the nuclear shape and shape coexistence in the exotic nucleus ^{80}Ge by IBM-2. In this study, we will discuss the properties of the low-lying states of ^{80}Ge, especially the relevant shape coexistence in the framework of IBM-2. Based on the fact that the relative energy of the d neutron boson is different from that of the proton boson, we calculate the energy levels of low-lying states, and the $B(E2)$ and $\rho^2(E0)$ transition strengths. We also compare the numerical results with the recent available experimental data. Then, we describe the shape coexistence phenomena in ^{80}Ge with IBM-2.

The structure of this paper is as follows. In Section 2, we briefly describe the Hamiltonian, $E2$ and $E0$ operators used in this study, and also present the criteria adopted for determining the IBM-2 model parameters. In Section 3, we compare the numerical results and experimental data and discuss the electromagnetic transition properties. Finally in Section 4, we give our summary and make some remarks.

2 Theoretical framework

In IBM-2, the total bosons include proton bosons and neutron bosons, satisfying $N=N_\pi+N_\nu$. The boson creation operators $s^+_{\rho,0}$ and $d^+_{\rho,\mu}$ and the corresponding annihilation operators $s_{\rho,0}$ and $d_{\rho,\mu}$ construct the generators of the group $U_\pi\otimes U_\nu$, where ρ represents π or ν and $\mu=-2,...,2$. The product $[N_\nu]\times[N_\pi]$ of symmetric representations of $U_\pi(6)$ and $U_\nu(6)$ constitutes the IBM-2 model space. The IBM-2 Hamiltonian used in this paper has the standard form [32]

$$\hat{H}=\varepsilon_{d\pi}\hat{n}_{d\pi}+\varepsilon_{d\nu}\hat{n}_{d\nu}+\kappa_{\pi\nu}\hat{Q}_\pi\cdot\hat{Q}_\nu+\omega_{\pi\pi}\hat{L}_\pi\cdot\hat{L}_\pi+\hat{M}_{\pi\nu}, \quad (1)$$

where $\hat{n}_{d\rho}=d^\dagger_\rho\cdot\tilde{d}_\rho$ stands for the d-boson number operator for neutrons ($\rho=\nu$) and protons ($\rho=\pi$), respectively. $\varepsilon_{d\rho}$ is the energy of the d-bosons relative to the s bosons. $\hat{Q}_\rho=(s^\dagger_\rho\tilde{d}_\rho+d^\dagger_\rho s_\rho)^{(2)}+\chi_\rho(d^\dagger_\rho\tilde{d}_\rho)^{(2)}$ denotes the quadrupole operator. χ_ρ in the quadrupole operator determines the type of deformation. The third term represents the quadrupole-quadrupole interaction between

proton bosons and neutron bosons with the strength parameter $\kappa_{\pi\nu}$. The fourth term of Eq. (1) denotes the dipole proton-proton interaction with strength $\omega_{\pi\pi}$, where $\hat{L}_\pi$ is the angular momentum operator, which can be explicitly expressed as $\hat{L}_\pi=\sqrt{10}[d^\dagger_\pi\cdot\tilde{d}_\pi]^{(1)}$. The last term denotes the Majorana interaction. Its explicit form is $\hat{M}_{\pi\nu}=\lambda_2(s^\dagger_\pi d^\dagger_\nu-s^\dagger_\nu d^\dagger_\pi)^{(2)}\cdot(s_\pi\tilde{d}_\nu-s_\nu\tilde{d}_\pi)^{(2)}$ $+\sum_{k=1,3}\lambda_k(d^\dagger_\pi d^\dagger_\nu)^{(k)}\cdot(\tilde{d}_\pi\tilde{d}_\nu)^{(k)}$, where the strength of Majorana interaction is embodied by the parameters λ_k (k=1,2,3).

The Hamiltonian in Eq. (1) gives rise to four dynamical symmetries $U_{\pi\nu}(5)$, $SU_{\pi\nu}(3)$, $O_{\pi\nu}(6)$, and $SU^*_{\pi\nu}(3)$, which correspond to a spherical, an axially symmetric, a γ-unstable, and a triaxial deformed shape respectively. For certain values of the model parameters, Eq. (1) can reduce to contain only one kind of dynamical symmetry [39]. The $B(E2)$ transition strengths and the $\rho^2(E0)$ values between 0^+ states could be used to search for the signatures of shape coexistence. In IBM-2, the $E2$ transition matrix element is defined as follows

$$B(E2,J\to J')=\frac{1}{2J+1}|\langle J'\|\hat{T}^{(E2)}\|J\rangle|^2, \tag{2}$$

where the $E2$ transition operator $\hat{T}^{(E2)}$ is given through the quadrupole operator Q_ρ as $\hat{T}^{(E2)}=e_\pi\hat{Q}_\pi+e_\nu\hat{Q}_\nu$. J and J' are the initial and final angular momenta, respectively. $e_\nu(e_\pi)$ represents the effective charge of neutron (proton) bosons; one can determine the effective charges by fitting the experimental data.

The $E0$ transition matrix element ρ in the IBM-2 is defined as

$$\rho(E0,J\to J')=\frac{Z}{eR^2}[\beta_{0\pi}\langle J'\|\hat{T}^{(E0)}_\pi\|J\rangle+\beta_{0\nu}\langle J'\|\hat{T}^{(E0)}_\nu\|J\rangle] , \tag{3}$$

where $R=1.2A^{1/3}$fm, and $\beta_{0\pi(\nu)}$ is the so-called proton (neutron) monopole boson effective charge in units of $e$fm^2. The $E0$ transition operator is written as $\hat{T}^{(E0)}=\beta_{0\pi}\hat{T}^{(E0)}_\pi+\beta_{0\nu}\hat{T}^{(E0)}_\nu=\beta_{0\pi}\hat{n}_{d\pi}+\beta_{0\nu}\hat{n}_{d\nu}$, where the $\hat{n}_{d\rho}$ is the same as in Eq. (1).

^{80}Ge is composed of N=48 neutrons and Z=32 protons, and is located at the Z=28, N=50 major shell. We take the doubly magic nucleus ^{78}Ni at Z=28 and N=50 as an inert core for the description of ^{80}Ge. In this case, there are two proton bosons outside the $Z=28$ shell, which are particle-like, while there is one neutron boson outside the N=50 shell in ^{80}Ge, which is hole-like. The microscopic picture demonstrates that the valence neutrons and protons occupy different orbitals when they are added to the $^{78}_{28}$Ni$_{50}$ core [4, 40]. The four valence protons are distributed among the fp orbitals. The two hole-like valence neutrons occupy the $g_{9/2}$ orbital [30, 40, 41]. In order to be consistent with the microscopic description and remove some of the degeneracies, we use different energies $\varepsilon_{d\pi}\neq\varepsilon_{d\nu}$ for d proton and neutron bosons, in the same way as in Refs. [36, 42]. In general, the parameters $\varepsilon_{d\rho}$ and $\kappa_{\pi\nu}$ are mainly used to reproduce the energy levels of low-lying states with positive parity. The values of $\varepsilon_{d\rho}$ mostly contribute to the spectrum of $U(5)$ nuclei. However, $\kappa_{\pi\nu}$ mainly characterizes the properties of deformed nuclei. The structure parameters χ_π and χ_ν in the quadrupole operators are used to describe the $B(E2)$ transition properties. Only the dipole interaction term $\hat{L}_\pi\cdot\hat{L}_\pi$ is explicitly considered in the Hamiltonian because there is only one hole-like neutron boson outside the N=50 shell in ^{80}Ge. $\hat{L}_\pi\hat{L}_\pi$ plays an important role on the description of rotational energy levels [43–45]. The parameter $\omega_{\pi\pi}$ can be used to tune the order of the 2^+_2 state and 4^+_1 state. The Majorana parameters mainly influence the mixed symmetry states. In order to reduce the number of free parameters in the Hamiltonian, for simplicity we take λ_2=0 and λ_1=λ_3 in this study.

The IBM-2 parameters are determined to reproduce the experimental data for ^{80}Ge: $\varepsilon_{d\pi}=0.315$MeV, $\varepsilon_{d\nu}=$ 1.080 MeV, $\kappa=-0.150$ MeV, $\chi_\pi=-1.200$, $\chi_\nu=0.900$, $\omega_{\pi\pi}=0.063$ MeV, and $\lambda_1=\lambda_3=0.800$ MeV in ^{80}Ge. We numerically diagonalized the IBM-2 Hamiltonian by the NPBOS code [46]. The IBM wave functions obtained are our starting point and can be used to compute the electromagnetic properties.

3 Results and discussion

The calculated results of the low-lying energy levels compared with the corresponding available experimental data are shown in Fig. 1. The experimental values are taken from Refs. [18, 30]. Each panel includes two different parts: the yrast band up to the 6^+ state and the nonyrast, low-spin, positive-parity levels. Figure 1 shows that the calculated energy levels from IBM-2 for the low-lying states agree very well with experimental data. The experimental energy levels of the yrast states are reproduced precisely by the theoretical calculations. The calculated ordering of the non-yrast states is consistent with the experimental data, although the theoretical prediction of the 2^+_2 state is lower than the experimental value. In particular, the calculated result of the first excited 0^+_2 state is almost equal to the experimental measurement of 639(1) keV, which is lower than the 2^+_1 state.

The energy ratio $R_{4/2}=E(4^+_1)/E(2^+_1)$ of the 2^+_1 state and 4^+_1 state is a well-known observable to measure the extent of quadrupole deformation. $R_{4/2}$ reaches the limit of 2.00 for $U_{\pi\nu}(5)$ dynamical symmetry (the spherical vibration), 2.50 for the $O_{\pi\nu}(6)$ dynamical symmetry (the γ-unstable rotor), and the maximum 3.33 for the $SU_{\pi\nu}(3)$ dynamical symmetry (the axial rotor) [39]. The experimental result for $R_{4/2}$ is 2.64 for ^{80}Ge, and the calculated value is 2.68. Both the experimental and theoretical value of $R_{4/2}$ predict that ^{80}Ge has a mostly typical γ-soft triaxial feature. At the same time, from Fig. 1 one

can see that both the experimental and calculated energy levels of the 2_2^+ state lie below the corresponding 4_1^+ state, and they form a pair of 2_2^+ and 4_1^+. This indicates that ^{80}Ge exhibits a characteristic of $O_{\pi\nu}(6)$ symmetry because the second 2^+ state lying below the 4_1^+ state is the manifestation of a γ-soft spectrum. However, the appearance of the 4_1^+ state at an energy of nearly 2.5 times that of the 2_1^+ level alone does not uniquely determine the $O_{\pi\nu}(6)$ structure [47]. In the $O_{\pi\nu}(6)$ limit of IBM-2, the 2_2^+ state and 4_1^+ state belong to the $\tau=2$ multiplet, but the 6_1^+, 0_2^+, 3_1^+, and 4_2^+ states belong to the $\tau=3$ multiplet. As a consequence, the 0_2^+ state ($\tau=3$ multiplet) is located at a much higher energy level and can decay to the second 2^+ state with $\tau=2$ rather than to the 2_1^+ state. However, the 0_2^+ state of ^{80}Ge actually lies at a lower energy level than the 4_1^+ and 2_2^+ states, even below the 2_1^+ level, both in experiment and theory. From the above discussion it is clear that ^{80}Ge is not a typical γ-soft nucleus, and at least deviates from the pure $O_{\pi\nu}(6)$ limit, although the yrast states show approximately the γ-soft rotor picture. More importantly, it is an important evidence of shape coexistence if a deformation state occurs near the almost spherical ground state or much lower than the first-excited 2^+ state [5]. Therefore, both the experimental and theoretical energy levels imply that shape coexistence occurs in ^{80}Ge.

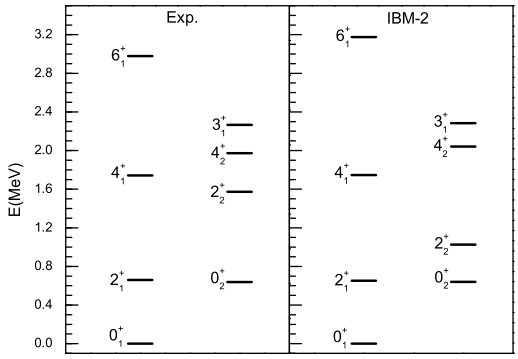

Fig. 1. The energy scheme for low-lying states of ^{80}Ge with positive-parity. The left-hand panel shows the experimental data and the right-hand panel the calculated result from IBM-2. The experimental energy levels are taken from Refs. [18, 30].

The $B(E2)$ transition probability and its branching ratios can also give important information on the nuclear structure. Unfortunately, only absolute $B(E2)$ transition strengths of $2_1^+ \to 0_1^+$, and $2_2^+ \to 0_1^+$ in ^{80}Ge have been observed so far. However, one can further explore shape coexistence in ^{80}Ge based on the other key sensitive quantities [47, 48]. To calculate the $E2$ transition strengths, the effective charges of proton and neutron bosons were determined to reproduce the experimental data of $B(E2,2_1^+ \to 0_1^+)$ and $B(E2,2_2^+ \to 0_1^+)$. By fitting the experimental data of the $B(E2,2_1^+ \to 0_1^+) = 200(26)$ $e^2\text{fm}^4$, we obtain $e_\nu = 13.9$ and $e_\pi = 6$ $e\text{fm}^2$ for ^{80}Ge. The effective charge of the neutron boson is much larger than the proton boson's, probably due to the effect of a valid proton midshell around $Z=34$. For the protons, the state space beyond the $Z=20$ shell closure and up to $Z=32-34$ is indeed made of the full pf shell [4], which might lead to a very valid proton subshell closure at Z=32 and 34. The other reason is that the parameters e_ν and e_π incorporate a (length)^2 factor, while the neutrons are occupying higher shells than protons in ^{80}Ge [49].

Table 1. Experimental and calculated $B(E2)$ values (in $e^2\text{fm}^4$) and $\rho^2(E0)$ values in ^{80}Ge. The experimental data are from Refs. [18, 30].

	$B(E2,2_1^+ \to 0_1^+)$	$B(E2,2_2^+ \to 0_1^+)$	$\rho^2(E0,0_2^+ \to 0_1^+)$
Exp.	200(26)	23(7)	
Cal.	200.0	21.3	0.001

The calculated $B(E2)$ transition strengths compared with the recent experimental values are listed in Table 1. The theoretical calculations are consistent with the experimental data. The calculated transition strength of $B(E2,2_2^+ \to 0_1^+)$ is in agreement with the experimental value within the experimental uncertainty. In the IBM, the key sensitive quantities $R_1 = B(E2,2_2^+ \to 2_1^+)/B(E2,2_1^+ \to 0_1^+)$ and $R_2 = B(E2,2_2^+ \to 0_1^+)/B(E2,2_2^+ \to 2_1^+)$ are usually considered as one of the most crucial available structure indicators [47] to distinguish the dynamical symmetry limits. The $U(5)$ symmetry is realized when $R_1 = 1.40$ and $R_2 = 0.011$, and the $O(6)$ symmetry when $R_1 = 0.79$ and $R_2 = 0.07$ [50]. The calculation result of $B(E2,2_2^+ \to 2_1^+)$ is 187.13 $e^2\text{fm}^4$. The calculated R_1 and R_2 are 0.94 and 0.11 respectively, which are much closer to $O(6)$ symmetry. Obviously, the predicted ratios of R_1 and R_2 are consistent with the character of the yrast states, but do not match the features of the non-yrast states. Thus, the above result has confirmed the existence of shape coexistence in ^{80}Ge.

One can obtain valuable information on the excited 0^+ states of different features coexisting in the same nucleus from the electric monopole transition strengths $\rho^2(E0)$ [51–53]. In order to further understand the properties of shape coexistence in ^{80}Ge, we calculate the $\rho^2(E0,0_2^+ \to 0_1^+)$ transition strength. Since experimental data about the $E0$ transition is still scarce in ^{80}Ge, we choose the parameters $\beta_{0\nu}$ and $\beta_{0\pi}$ as the values derived in Ref. [54] from a detailed analysis of $E0$ transition in $O(6)$-like nuclei, namely, $\beta_{0\nu}=0$ and $\beta_{0\pi}=0.20$ $e\text{fm}^2$. The calculated transition strength is also listed in Table 1. Because the $E0$ operator is proportional to $\hat{n}_d$, no $E0$ transitions occur in the $U(5)$ dynamical limit [55].

Within the $O(6)$ limit, the selection rules are $\triangle\sigma=0,\pm2$, $\triangle\tau=0$, so the $0_2^+\rightarrow0_1^+$ transition is forbidden [56]. The present calculated value of $\rho^2(E0)$ is comparable with those observed in ^{72}Ge, ^{102}Pd and ^{120}Xe [51, 56], which implies that different nuclear shapes coexist in ^{80}Ge.

Furthermore, the choice of the parameters to reproduce the properties of the low-lying states might give us a clue to understand shape coexistence in nuclei. Recalling the best fit parameters in the present calculation, we found that the $\varepsilon_{d\rho}$ is much larger than $\kappa_{\pi\nu}$, which reflects that ^{80}Ge mainly exhibits the characteristics of spherical vibration or $U(5)$ dynamical symmetry. At the same time, the structure parameter of the quadrupole operator $\chi_\pi=-1.200$, and $\chi_\nu=0.900$ were adopted in this paper. The sum $\chi_\pi+\chi_\nu=-0.3$ indicates that the ^{80}Ge nucleus is close to the $O(6)$ dynamical symmetry or γ-soft in IBM. As mentioned above, combining the information from the best fit parameters and the properties of the low-lying states, the physical picture from the IBM point of view is clear: both collective spherical and γ-soft vibration structures coexist in ^{80}Ge. Microscopically, the recent shell model calculations in the $pfgd$ model space suggest that tensor forces play an important role in setting up a shape coexistence environment and the tensor effect changes dynamically with orbital occupation and spin [57]. For ^{80}Ge, many neutrons occupying the $g_{9/2}$ orbital reduce the proton $f_{7/2}-f_{5/2}$ gap, so much more particle-hole excitations occur over the gap, which lead to much stronger shell evolution [58]. Other studies have clearly shown that the $\nu s_{1/2}$ shell drops in energy and becomes almost degenerate with the lower-lying $\nu d_{5/2}$ shell at $Z=32$ [18]. Therefore, neutron pair excitations across $N=50$ are likely to include both orbitals, which results in significant configuration mixing. The deformation and change of shell structure driven by the combination of the tensor forces and changes of major configurations can occur and can enhance shape coexistence in ^{80}Ge.

4 Conclusion

In summary, we have discussed the properties of the low-lying states, especially the relevant shape coexistence, in ^{80}Ge, which is near one of most neutron-rich doubly magic nuclei at $N=50$ and $Z=28$. Based on the different relative energy for d proton bosons and neutron bosons, *i.e.*, $\varepsilon_{d\pi}\neq\varepsilon_{d\nu}$, the low-lying positive parity states agree very well with experimental data in IBM-2. More importantly, the calculated energy level of the first excited 0_2^+ state, which is associated with the shape coexistence phenomenon, is almost equal to the experimental value at 659 keV, which is lower than the 2_1^+ state. Both the experimental and theoretical energy spectrum indicate that shape coexistence exists in the ^{80}Ge structure, although the value of the characteristic ratio of $R_{4/2}$ suggests that ^{80}Ge has mostly typical γ-soft triaxial features.

The calculated $B(E2)$ transition strengths agree with the experimental data within the experimental uncertainty. The key sensitive quantities do not match with the features of the non-yrast states, which demonstrates a different property of ^{80}Ge compared with its energy spectrum structure. Therefore, the above result has just confirmed the existence of shape coexistence in ^{80}Ge. Furthermore, the $\rho^2(E0,0_2^+\rightarrow0_1^+)$ transition strength has been calculated. The theoretical result of the $\rho^2(E0,0_2^+\rightarrow0_1^+)$ transition also indicates that different nuclear shapes exist at the same time in ^{80}Ge.

The best fit values of $\varepsilon_{d\rho}$ are much larger than $\kappa_{\pi\nu}$, which implies that ^{80}Ge has the property of $U(5)$ dynamical symmetry, while the sum $\chi_\pi+\chi_\nu=-0.3$ indicates that ^{80}Ge is close to γ-soft or $O(6)$ dynamical symmetry in IBM. Combining the results of the best fit parameters in the present calculations and the properties of the low-lying states, we find that both collective spherical and γ-soft vibration structures coexist in ^{80}Ge from the IBM point of view. However, experimental information on $E2$ and $E0$ transitions from the 0_2^+ state to other states in ^{80}Ge is still scarce. As a result, our theoretical analysis for the associated 0_2^+ level might be incomplete. More theoretical calculations and experimental investigations on these aspects are needed.

We thank Profs. Y. X. Liu, G. L. Long and C. W. Shen for helpful discussions.

References

1 A. Poves, J. Phys. G: Nucl. Part. Phys., **43**: 020401 (2016)
2 K. Heyde and J. L. Wood, Rev. Mod. Phys., **83**: 1467 (2011)
3 A. Gade and S. N. Liddick, J. Phys. G: Nucl. Part. Phys., **43**: 024001 (2016)
4 F. Nowacki, A. Poves, E. Caurier, and B. Bounthong, Phys. Rev. Lett., **117**: 272501 (2016)
5 A. N. Andreyev, Nature, **405**: 430 (2000)
6 A. Görgen and W. Korten, J. Phys. G: Nucl. Part. Phys., **43**: 024002 (2016)
7 Y. X. Liu, S. Y. Yu, and Y. Sun, Sci. China-Phys. Mech. Astron., **58**: 112003 (2015)
8 G. X. Dong, X. B. Wang, and S. Y. Yu, Sci. China-Phys. Mech. Astron., **58**: 112004 (2015)
9 Z. J. Bai, X. M. Fu, C. F. Jiao, and F. R. Xu, Chin. Phys. C, **39**: 094101 (2015)
10 J. Sun, T. Komatsubara, J. Q. Wang, H. Guo, X. Y. Hu, Y. J. Ma, Y. Z. Liu, and K. Furuno, Chin. Phys. C, **40**: 124001 (2016)
11 F. Iachello, N. V. Zamfir, and R. F. Casten, Phys. Rev. Lett., **81**: 1191 (1998)
12 Y. X. Liu, L. Z. Mu, and H. Q. Wei, Phys. Lett. B, **633**: 49 (2006)

13 M. Hasegawa, K. Kaneko, T. Mizusaki, and Y. Sun, Phys. Lett. B, **656**: 51 (2007)
14 Y. Sun et al, Phys. Rev. C, **80**: 054306 (2009)
15 Y. X. Liu, Y. Sun, X. H. Zhou, Y. H. Zhang, S. Y. Yu, Y. C. Yang, H. Jin, Nucl. Phys. A, **858**: 11 (2011)
16 Z. Z. Ren, Phys. Rev. C, **65**: 051304 (2002)
17 G. Hagen, G. R. Jansen, and T. Papenbrock, Phys. Rev. Lett., **117**: 172501 (2016)
18 A. Gottardo et al, Phys. Rev. Lett., **116**: 182501 (2016)
19 E. Padilla-Rodal et al, Phys. Rev. Lett., **94**: 122501 (2005)
20 S. F. Shen, S. J. Zheng, F. R. Xu, and R. Wyss, Phys. Rev. C, **84**: 044315 (2011)
21 D. L. Zhang and B. G. Ding, Chin. Phys. Lett., **30**: 122101 (2013)
22 D. L. Zhang, and C. F. Mu, Sci. China-Phys. Mech. Astron., **61**: 012012 (2018)
23 M. Lettmann et al, Phys. Rev. C, **96**: 011301 (2017)
24 H. Iwasaki et al, Phys. Rev. C, **78**: 021304 (2008)
25 S. Mukhopadhyay et al, Phys. Rev. C, **95**: 014327 (2017)
26 L. Guo, J. A. Maruhn, and P. G. Reinhard, Phys. Rev. C, **76**: 034317 (2007)
27 P. Sarriguren, Phys. Rev. C, **91**: 044304 (2015)
28 T. Nikšić, P. Marević, and D. Vretenar, Phys. Rev. C, **89**: 044325 (2014)
29 G. H. Bhat, W. A. Dar, J. A. Sheikh, and Y. Sun, Phys. Rev. C, **89**: 014328 (2014)
30 D. Verney et al, Phys. Rev. C, **87**: 054307 (2013)
31 S. T. Hsieh, H. C. Chiang, and D. S. Chuu, Phys. Rev. C, **46**: 195 (1992)
32 F. Iachello, and A. Arima *The Interacting Boson Model* (Cambridge, England: Cambridge University Press, 1987)
33 P. D. Duval, D. Goutte, and M. Vergnes, Phys. Lett. B, **124**: 297 (1983)
34 J. P. Elliott, J. A. Evans, V. S. Lac, and G. L. Long, Nucl. Phys. A, **609**: 1 (1996)
35 K. Nomura et al, Phys. Rev. C, **95**: 064310 (2017)
36 D. L. Zhang and B. G. Ding, Sci. China-Phys. Mech. Astron., **57**: 447 (2014)
37 D. L. Zhang and C. F. Mu, Chin. Phys. Lett., **33**: 102102 (2016)
38 D. L. Zhang and C. F. Mu, Sci. China-Phys. Mech. Astron., **59**: 682012 (2016)
39 P. Cejner, J, Jolie, and R. F. Casten, Rev. Mod. Phys., **82**: 2155 (2010)
40 G. Gürdal et al, Phys. Rev. C, **88**: 014301 (2013)
41 H. Rotter et al, Nucl. Phys. A, **514**: 401 (1990)
42 H. Dejbakhsh, D. Latypov, G. Ajupova, and S. Shlomo, Phys. Rev. C, **46**: 2326 (1992)
43 K. Nomura, T. Otsuka, N. Shimizu, and L. Guo, Phys. Rev. C, **83**: 041302 (2011)
44 K. Nomura, T. Otsuka, and P. V.Isacker, J. Phys. G: Nucl. Part. Phys., **43**: 024008 (2016)
45 D. L. Zhang and C. F. Mu, Sci. China-Phys. Mech. Astron., **60**: 042011 (2017)
46 T. Otsuka and N. Yoshida, Program NPBOS, JAER-M Report, No.85 (unpublished): (1985)
47 R. F. Casten and D. D. Warner, Rev. Mod. Phys., **60**: 389 (1988)
48 D. L. Zhang, S. Q. Yuan, and B. G. Ding, Chin. Phys. Lett., **32**: 062101 (2015)
49 W. D. Hamilton, A. Irback, and J. P. Elliott, Phys. Rev. Lett., **53**: 2469 (1984)
50 J. Stachel, P. Van Isacker, and K. Heyde, Phys. Rev. C, **25**: 650 (1982)
51 P. F. Mantica and W. B. Walters, Phys. Rev. C, **53**: R2586 (1996)
52 E. Bouchez et al, Phys. Rev. Lett., **90**: 082502 (2003)
53 B. A.Brown, A. B. Garnsworthy, T. Kibédi, and A. E. Stuchbery, Phys. Rev. C, **95**: 011301 (2017)
54 B. R. Barrett and T. Otsuka, Phys. Rev. C, **46**: 1735 (1992)
55 A. Leviatan and D. Shapira, Phys. Rev. C, **93**: 051302 (2016)
56 J. L. Wood, E. E. Zganjar, C. E. Coster, and K. Heyde, Nucl. Phys. A, **651**: 323 (1999)
57 K. Kaneko, Y. Sun, and R. Wadsworth, Phys. Scr. **92**: 114008 (2017)
58 Y. Tsunoda et al, Phys. Rev. C, **89**: 031301(R) (2014)